Met. Mater. Int., Vol. 22, No. 4 (2016), pp. 670~680
doi: 10.1007/s12540-016-5687-4

Interface Morphology and Mechanical Properties of Al-Cu-Al Laminated Composites Fabricated by Explosive Welding and Subsequent Rolling Process

M. M. Hoseini-Athar and B. Tolaminejad*

Department of Metallurgy and Materials Engineering, Faculty of Engineering, University of Kashan, Kashan 8731753153, Iran

(received date: 16 December 2015 / accepted date: 5 March 2016)

Explosive welding is a well-known solid state method for joining similar and dissimilar materials. In the present study, tri-layered Al-Cu-Al laminated composites with different interface morphologies were fabricated by explosive welding and subsequent rolling. Effects of explosive ratio and rolling thickness reduction on the morphology of interface and mechanical properties were evaluated through optical/scanning electron microscopy, micro-hardness, tensile and tensile-shear tests. Results showed that by increasing the thickness reduction, bonding strength of specimens including straight and wavy interfaces increases. However, bonding strength of the specimens with melted layer interface decreases up to a threshold thickness reduction, then rapidly increases by raising the reduction. Hardness Values of welded specimens were higher than those of original material especially near the interface and a more uniform hardness profile was obtained after rolling process.

Keywords: explosive welding, rolling composite, interface, hardness test

1. INTRODUCTION

In recent years, composite materials produced from metallic layers have become increasingly popular for engineering applications due to their enhanced mechanical properties, better corrosion resistance, high electrical conductivity, cost effectiveness, etc. [1,2]. Laminated sheets consisting of aluminum and copper layers are intermediate products for manufacturing of connectors, armored cables, bus bars and heating conductive elements with the advantage of reduced weight [3].

Conventional fusion welding methods cannot be used for joining Al to Cu because of their huge differences in physical and chemical properties [4]. Moreover, formation of microcracks and brittle intermetallic compounds (IMCs) are highly expected in fusion welded joints. IMCs with thickness above 5 μm seriously deteriorate the mechanical properties. These problems have persuaded the researchers and industries to extend their welding methods into solid state procedures [5]. Therefore, solid state welding techniques such as cold roll welding [6,7], diffusion bonding [8], friction welding [9] and explosive welding/cladding [10] have been developed as the alternative processes.

For many years, explosive welding has been used for successful production of laminated composites made of various materials. This method involves a fast bond between two or more layers as a result of a high speed oblique collision of materials to be joined by the detonation of an explosive charge placed on top of the flyer plate [11]. Figure 1 depicts a typical parallel setup for the explosive welding.

The main theories suggested for wave formation in explosive welding include indentation, flow instability, vortex shedding and stress wave mechanisms [12]. Bahrani *et al*. [13] stated that indentation of the re-entrant jet into the parent plate leads to formation of a hump which periodic formation of them is responsible for wavy interface. Considering the Kelvin-Helmholtz instability, another mechanism was published [14] based on the fact that whenever two fluids with different velocities interact, instabilities occur at the interface due to the turbulent flow. Cowan *et al*. proposed a mechanism based on the analogy between the interfacial waves in explosive welding and von Karman's vortex streets generated behind an obstacle [15]. Another theory indicates that compressive stress waves are generated at the collision point and reflected at the free surface of the base plate causing periodic interferences at the interface of the plates [16]. Earlier studies [10,17] revealed that the wave amplitude of the interface is dependent on the impact energy and by controlling it, transition from wavy to straight or wavy with melted layer interfaces could take place. There is no consensus on mentioned theories, however recent observations have shown that indentation mechanism governs the low collision angle (<~20°) condition while Kelvin-Helm-

*Corresponding author: tolaminejad@kashanu.ac.ir

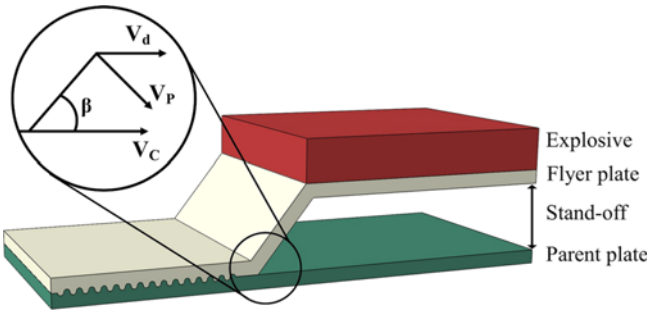

Fig. 1. Schematic representation of the parallel arrangement for explosive welding.

holtz instability may happen for metals with low shear strength under large collision angles (> ~30°) [11].

Similar to other welding methods, the explosive welded interface strongly depends on careful selection of process parameters. These parameters include surface preparation, plate separation or stand-off distance, explosive load/ratio, initial and dynamic collision angles, flyer plate velocity, and detonation and collision velocities. The proper parameter selection is done based upon the mechanical properties, density and shear wave velocity of each material [18].

Effect of different welding parameters on interface morphology and properties of the joint have been widely studied. Acarer *et al*. [19] reported that an increase in stand-off distance and explosive loading cause a wavy structure at the interface. Durgutlu *et al*. [20] showed that wavelength and amplitude of the waves are getting higher with increasing the stand-off distance. In some researches, it is believed that wavy interface offers better bonding strength [21,22]. On the other hand, Rajani and Mousavi [23] investigated the dependency of metallurgical and mechanical interfacial characteristics on explosive welding parameters such as explosive ratio and stand-off distance. They observed that by raising the mentioned parameters, locally melted zones appear at the interface. Hokomato *et al*. [24] have stated that the kinetic energy dissipated by collision causes the melting at the interfacial zone and formation of intermetallic compounds. According to Inal and Zimmerly [25], intermetallic compounds in the welding interface reduce the ductility and bonding strength. Kacar and Acarer [26] studied the bonding strength of different materials after explosive welding and proved that the tensile-shear strength across the interface of many metal combinations is higher than the strength of the weaker component.

After welding, a subsequent forming process is usually employed in order to manufacture near-net-shape components [27]. Mamalis *et al*. [28] investigated the effect of cold rolling on explosively welded strips and fabricated sound trimetallic strips with sufficient strength and bonding integrity. Asemabadi *et al*. [29] evaluated the cold rolling of Al-Cu joints without considering the effect of different morphologies and reporting the details of tensile-shear strength. Moreover, explosive welding followed by multi-pass extrusion has resulted in perfect bimetallic rods [30].

Although prediction of welding interface is possible based on the initial parameters and explosive welding window [18], many researchers have stated that different morphologies may be obtained in different regions of the welded plates due to the unstable nature and lack of control of explosion process [31]. Therefore, it seems necessary to investigate the effect of subsequent rolling process on different types of welding morphology.

In this paper, explosive welding parameters were set in a way to achieve straight, wavy and melted layer interface morphologies according to the Al-Cu welding window calculated by authors elsewhere [17]. Rolling process was applied to as-welded specimens under different thickness reductions. Microscopic studies and mechanical tests were carried out to investigate the effect of rolling process on the interface morphology and strength of welded plates.

2. EXPERIMENTAL PROCEDURE

Laminated composites consisted of copper-10100 layer in the middle with aluminum-1100 layers on both sides were manufactured by double explosive welding process using parallel arrangement (Fig. 2(a)). The dimensions of each plate were 400×200×5 mm^3. ANFO-6% fuel oil with detonation velocity of 2400 m/s was employed as explosive material. In order to investigate the effects of explosive ratio (ratio of explosive mass to the mass of the flyer plate, R) on the bonding interface, three different R values of 1, 1.6 and 2.2 were selected. The initial gap between two metal plates was chosen to be about 2.5 mm. After explosive welding, strips with dimensions of 70×40×15 mm^3 cut from the laminated plates, were cold rolled at thickness reductions (r) equal to 15, 30, 45, 55, 65 and 80% (Fig. 2(b)). Rolling process was performed on an experimental 2-high rolling mill at a constant speed of 15 rpm between two steel rolls of 150 mm diameter.

To reveal the interface morphology, specimens cut parallel to the detonation and rolling direction were ground with emery papers up to grade number 3000 and were polished with alumina. Then, a Meiji ML7100 optical microscope (OM) was used for microscopic examination of the interface. Also, metallographic images were processed by JMicroVison analyzing software to measure the interface length.

For evaluating the mechanical properties of laminated composites, microhardness, tensile and tensile-shear tests were performed. Hardness variation profiles were measured across the thickness using Matsuzawa vickers microhardness testing machine with a test load of 100 gf and duration of 15 s. Tensile tests were done according to ASTM-E8M with a crosshead speed of 10^{-4} m/s. Tensile specimens were prepared parallel to the rolling direction (Fig. 3(a)).

Tensile-shear tests were conducted based on ASTM D3165 using a GUNT WP310 universal testing machine. Figure 3(b)

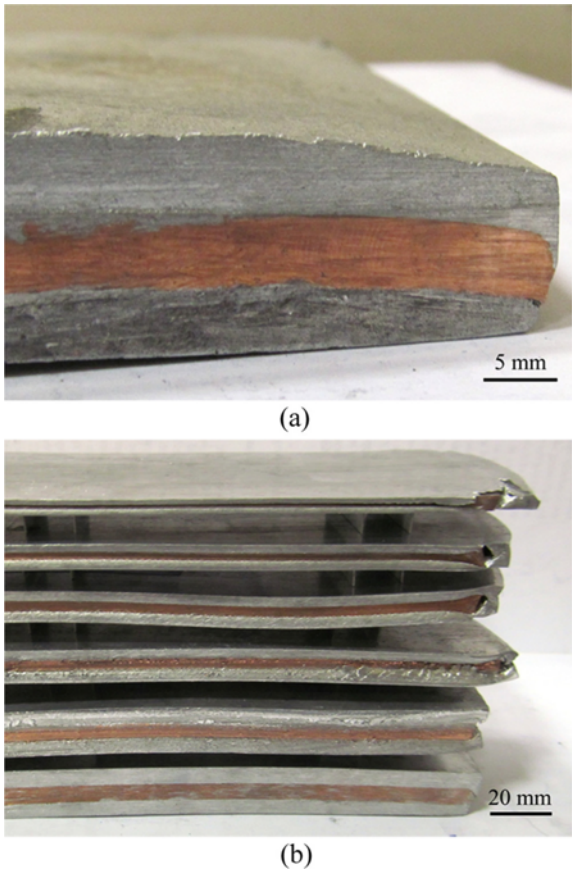

Fig. 2. Laminated composites fabricated by explosive welding (a) before and (b) after cold rolling under different thickness reductions.

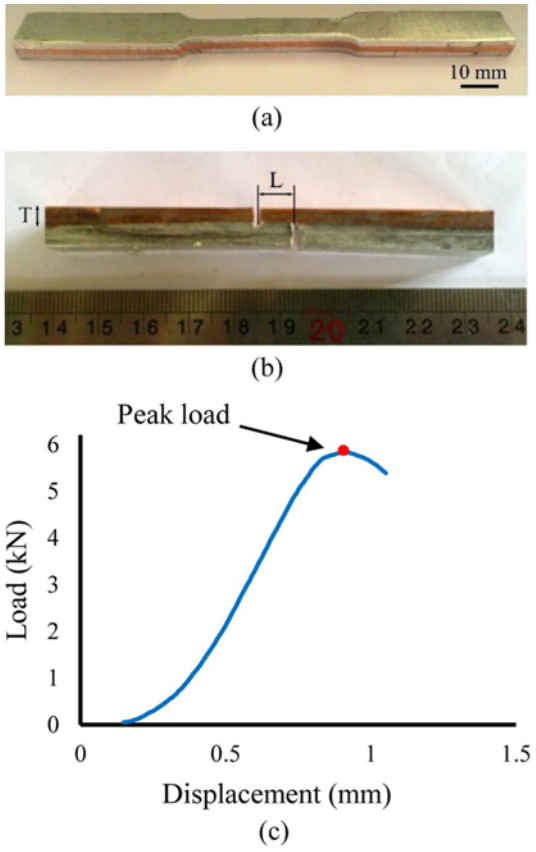

Fig. 3. (a) Tensile test specimen cut from Al-Cu-Al laminated composite, (b) tensile-shear specimen before performing the test, and (c) schematic load-displacement curve corresponding to the tensile-shear test.

demonstrates the tensile-shear specimen before performing the test. According to standard test method, in order to prevent exceeding the yield point of the metal in tension during test, the maximum permissible length of overlapped portion (L) may be computed from the following equation:

$$L = \sigma_y \frac{T}{\tau} \quad (1)$$

where σ_y is the yield point of softer material, T is the thickness and τ should be considered as 1.5 times higher than the estimated average shear bonding strength. This equation ensures that bond separation occurs sooner than bulk material failure. The shear strength of the joint is defined as the peak shearing load (Fig. 3(c)) divided by the overlapped area.

A Phillips XL scanning electron microscope (SEM) equipped with energy dispersive spectrometer (EDS) was used to identify the intermetallic compounds and also examine the fracture surfaces of tensile and tensile-shear test specimens.

3. RESULTS AND DISCUSSION

3.1. Microscopic observations

Figure 4 shows a set of optical micrographs of as-welded specimen interfaces. As it can be seen in Fig. 4(a), a smooth interface with only traces of intermetallics is obtained in the case of using low explosive ratio (R=1). During the process, surface contamination is forced out of the impact area by high pressures generated via explosion. By increasing the explosive ratio to R=1.6, interface transforms to a wavy state with wavelength and amplitude of 400 μm and 100 μm, respectively (Fig. 4(b)). It has been shown that the wavelength and amplitude increase by increasing the explosive ratio [18]. This is because of higher collision speed and impact pressure which in turn results in higher plastic deformation at the interface [32]. On the other hand, by further increasing the explosive ratio to R=2.2, a poor asymmetrical wavy interface with irregular morphology and significant amounts of intermetallics is formed (Fig. 4(c)) which is also characterized by the presence of cracks and solidification defects such as cooling cavities (Fig. 5). These compounds are a consequence of partial melting at the interface due to the adiabatic heating of trapped jet inside vortices of the waves [18] or dissipation of kinetic energy of the impacting plates in the form of heat (causing local melting) [24]. When melting occurs at the vortices, it results in circular movement and vigorously stirring of molten materials which leads to intermixing of Al and Cu and formation of IMCs owing

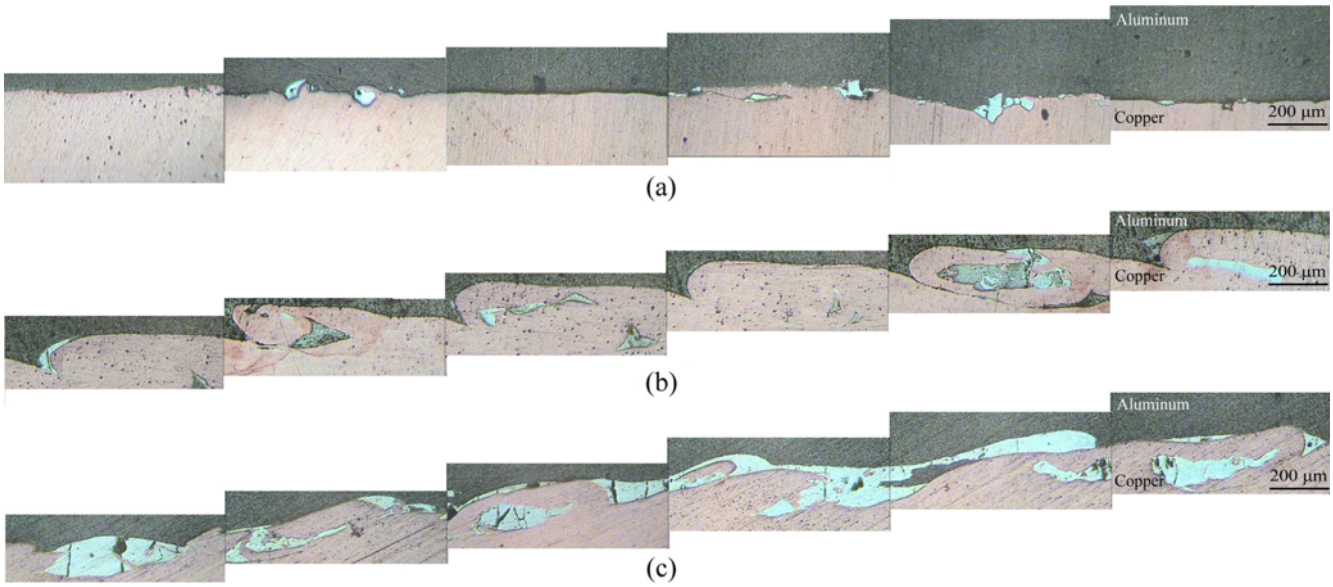

Fig. 4. Morphology of weld interface for different explosive ratios: (a) R=1, (b) R=1.6, and (c) R=2.2.

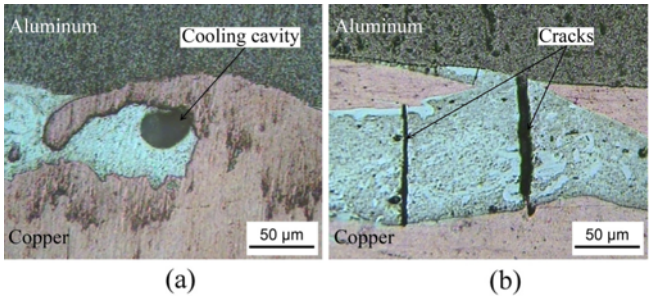

Fig. 5. Typical defects observed in explosively welded joints: (a) cooling cavity and (b) cracking.

to the high affinity of these metals. According to Hokamoto *et al*. [24] by increasing the explosive ratio and consequently the plate velocity, dissipated energy in the form of heat increases which leads to a higher amount of molten zones. The material near a vortex of the welded joint is heated the most, so intermetallic compounds are usually more expected in the wave vortices. On the other hand, the molten zone is surrounded by cold metal and subjected to a very high cooling rates of the order of 10^5–10^7 K/s [33]. Rapid solidification at the vortices is the main reason for cooling cavities and cracks. These defects can deteriorate the properties of bonding interface [19].

EDS analysis of the local melted zones confirms the formation of Al_2Cu intermetallics at the interface (Fig. 6). It seems that increasing the explosive ratio has no effect on the composition of the intermetallic phase. This may be because Al_2Cu has the lowest heat of formation (-6.1 $kJ.mol^{-1}$) among Al-Cu intermetallics which indicates that this compound most readily appears at the interface [34].

To investigate the effect of rolling process, interface morphology of the specimens after different thickness reductions

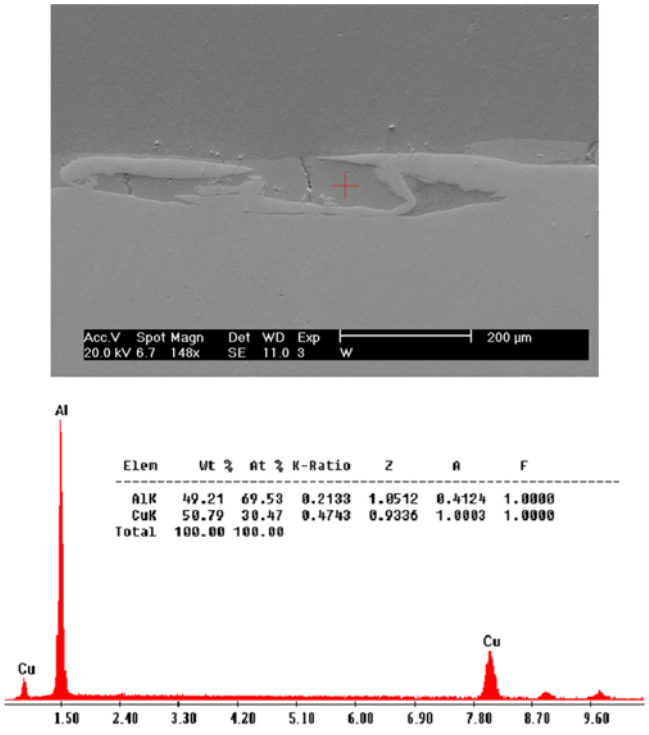

Fig. 6. EDS analysis obtained from the melted zone.

were examined. Metallographic observations revealed that although local flattening of waves are seen, but no significant interfacial change takes place after rolling of specimens welded using R=1 (Figs. 7(a) and (b)). This is due to the almost smooth initial morphology of the interface in this case.

Flattening of the vortices under compressive stress applied during rolling can be observed more clearly for specimens welded with explosive ratio of R=1.6. Comparing Figs. 4(b),

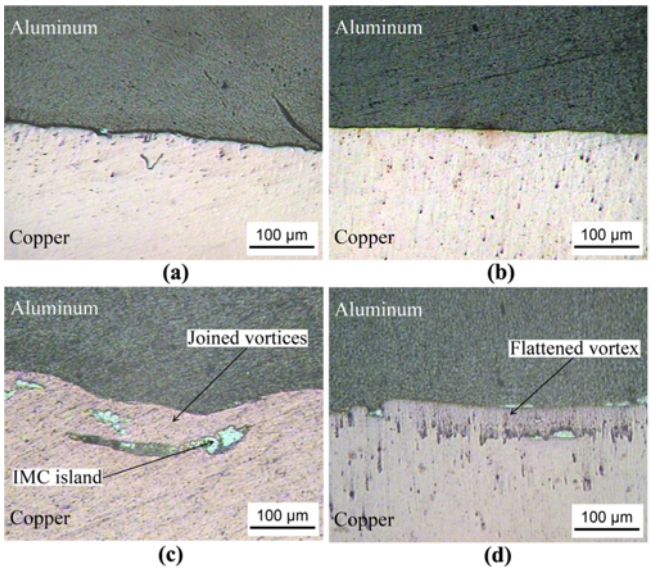

Fig. 7. Morphology of the weld interface after explosive welding with R=1 and rolling at thickness reduction of (a) 15% and (b) 30%; with R=1.6 and rolling at thickness reduction of (c) 30% and (d) 65%.

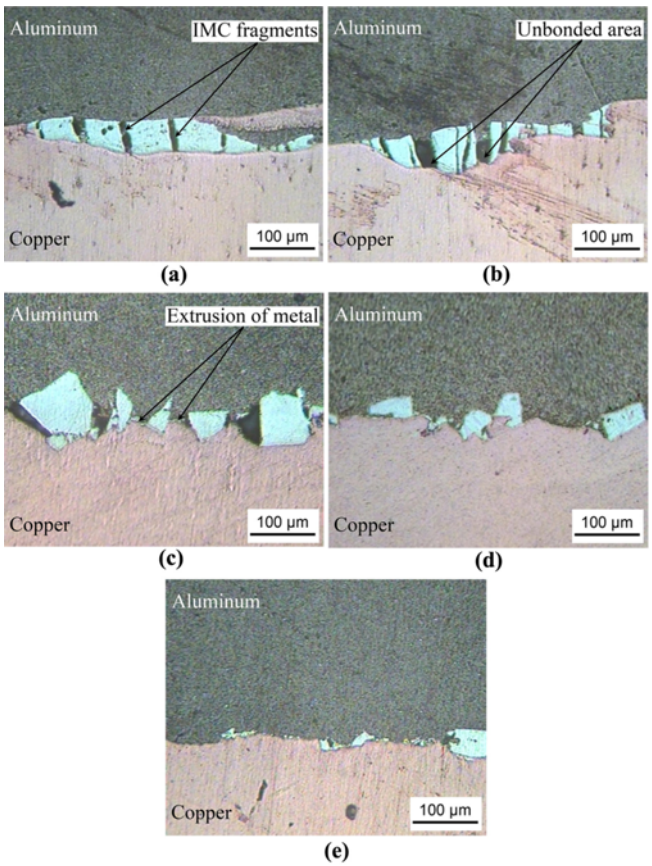

Fig. 8. Morphology of the interface after explosive welding with R=2.2 and rolling at thickness reductions of (a) 15%, (b) 30%, (c) 45%, (d) 65%, and (e) 80%.

7(c) and (d) indicates that after rolling process, interface becomes less wavy. This flattening along with joining of adjacent vortices leads to the formation of entrapped islands and consequently the relocation of IMCs away from the interface. By increasing the thickness reduction up to r=65%, an almost straight interface is achieved. Mamalis *et al*. have reported similar observations for trimetallic strips [35].

Figure 8 demonstrates the effect of rolling process on the morphology of the specimens welded under highest explosive ratio (R=2.2). During rolling, fracture of intermetallic compounds into smaller fragments occurs at the interface (Fig. 8(a)). By increasing the thickness reduction, fragmentation is intensified and small fragments get further away from each other. This causes appearing of cracks and unbonded areas (such as voids) between IMC fragments (Fig. 8(b)). However, no void is observed between fragments at thickness reductions higher than r=45%. Indeed, metals are completely extruded through the cracks between intermetallics giving rise to formation of secondary bonds between aluminum and copper similar to the film theory suggested by Vaidyanath *et al*. [36] as the main mechanism of cold roll bonding (CRB). The extrusion of underlying virgin metals of opposing plates are appropriate for metal-to-metal bonding within a few interatomic distances [37]. For dissimilar components, the extrusion of the softer metal through cracks in the intimate surface is always easier than the extrusion of the harder metal counterpart. Based on previous evidence, there is a threshold thickness reduction necessary for surface layer break up and establishment of new bonds [38]. Also, the existing tongue-groove joint might improve the bonding via mechanical locking. By increasing the thickness reduction above r=45%, IMC fragments become smaller and the extrusion path required for creation of bonds becomes shorter. This might lead to better filling of cracks and consequently better bonding properties.

On the other hand, the initial bonded area shifts to the entrance of the roll gap by increasing the thickness reduction. It means that the time of loading by normal pressure on the interface becomes longer [39,40]. Therefore, it can be predicted that the bond strength will be raised with increasing the total deformation [41]. At high r value, flattening of waves and IMC fragmentation continues so that under rolling reduction of about r=80%, an almost smooth interface is obtained.

For correlating the effects of rolling on interface morphology with bonding strength, a quantified parameter, i.e. effective bond length (L_{eff}) was introduced. In this regard, a 10 mm interval of the interface was examined quantitatively. Schematic representation of L_{eff} and related quantities are shown in Fig. 9(a). This parameter is an indicative of the length of Al-Cu interface (which is preferred to the weak Al/Cu-IMC interface) and is defined as follows:

$$L_{eff} = \frac{\text{length of Al}-\text{Cu interface}}{\text{total length of interface}} \times 100 \quad (2)$$

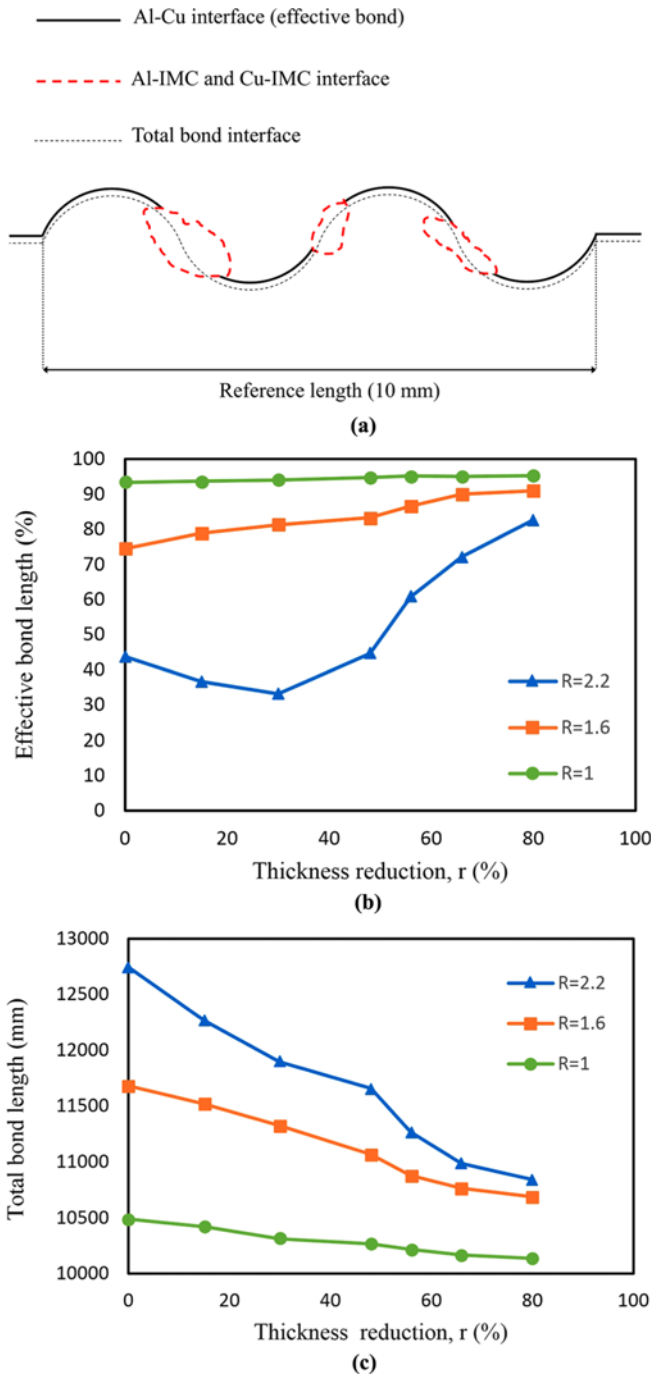

Fig. 9. (a) Schematic representation of quantitative interface parameters; variation of (b) effective and (c) total bond length as a function of rolling thickness reduction.

Total length of interface (L_t) includes Al-Cu, Al-IMC and Cu-IMC interfaces and also local unbonded areas (voids between IMC fragments in Fig. 8(a) and (b)). In fact, because the interface has wavy morphology, the total length of interface in the mentioned interval is more than 10 mm. According to earlier investigations, higher bond length can improve the bonding strength if IMCs are not present at the interface [10]. The effects of rolling thickness reduction on the L_{eff} and L_t for different welding interfaces are plotted in Figs. 9(b) and (c).

Referring to Figs. 8 and 9, it is clearly seen that the specimen welded under explosive ratio of R=1 has the highest L_{eff} value due to the lowest amount of IMCs and defects at the interface. On the other hand, increasing the explosive ratio results in the reduction of effective bond length due to the formation of intermetallic compounds. However, L_t increases with increasing the R value.

For R=1.6, L_{eff} slightly increases with increasing the thickness reduction. This is arising from the fragmentation of IMCs and their movement away from the interface because of joining of vortices and formation of intermetallic islands. Nevertheless, owing to the small amounts of IMCs at the interface, increasing of L_{eff} is not very significant. Rolling process reduces the total bond length by straightening the waves. Although interfaces of R=1.6 and R=2.2 specimens have higher L_t (as a result of wavy interface), but L_{eff} values for these specimens is much lower than those of R=1 specimen.

For R=2.2, L_{eff} decreases up to thickness reduction of about r=30%. This observation can be explained by the fracture of large IMCs at the interface and getting away from each other which cause formation of local unbonded areas as voids between fragments (Figs. 8(a) and (b)). Creation of these areas results in reduction of Al-Cu interface and L_{eff}. By further increasing the thickness reduction, new bonding areas are formed via onset of extrusion of virgin metals through the voids and compensate the reduced value of L_{eff} (Fig. 8(c)). Also, beyond r=45%, increasing the thickness reduction brings about an additional distance between IMC fragments and formation of bonds at the distance between them which increases the effective bond length.

The copper layer near the interface was etched to investigate the effect of explosive welding and subsequent rolling on the microstructure. Optical microscopy demonstrates that excessive grain refinement occurs at the interface and grains are elongated in direction of the explosion. This is due to the increase of tangential component of impact velocity and the shearing stresses produced between the impacting metals which induces a high level of plastic deformation [18]. Comparing Figs. 10(a) and (b) indicates that increasing the explosive ratio not only alters the interface morphology, but also increase the width of severely deformed layer at the interface. After rolling process, a banded microstructure is obtained (Fig. 10(c)). However, this structure is less obvious near the interface due to the prior hardening during explosive welding.

3.2. Microhardness measurements

Microhardness variation profiles through the thickness of Al-Cu-Al plates after welding under different explosive ratios are presented in Fig. 11(a). It is evident from this figure that during explosive welding, both parent and flyer plates expe-

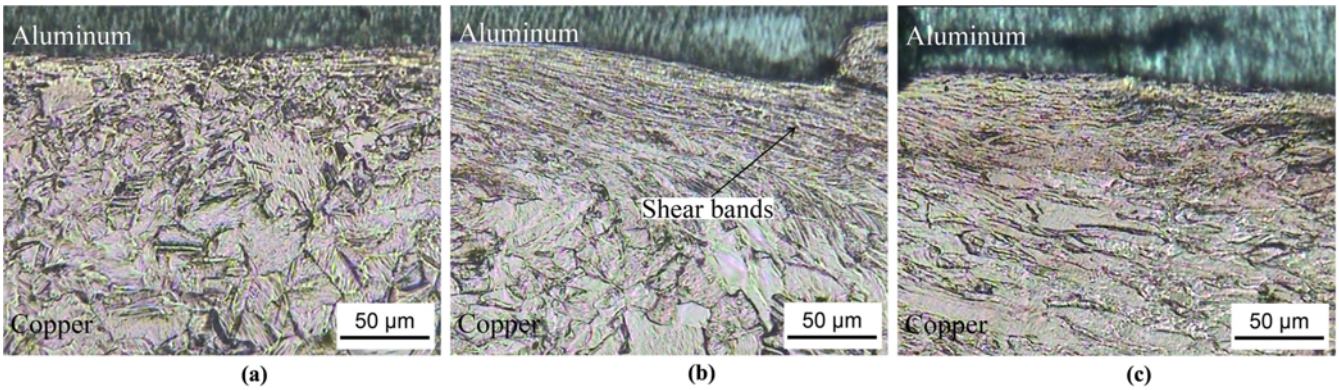

Fig. 10. Microstructure of copper after explosive welding using explosive ratio of (a) R=1, (b) R=1.6, and (c) R=1.6 and subsequent rolling with thickness reduction of r=55%.

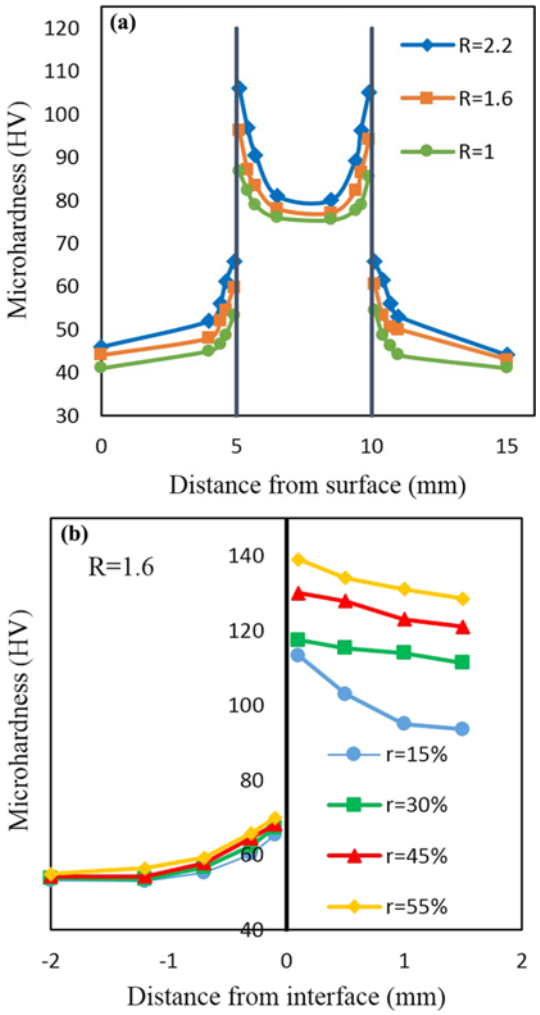

Fig. 11. Variations of hardness after explosive welding (a) using different explosive ratios and (b) using R=1.6 followed by rolling under different thickness reductions.

rience a hardness increase from the initial values of 30 and 74 vickers for Al and Cu, respectively. The highest microhardness is observed near the welding interface. The reason for the increase of hardness of the joint is the plastic deformation due to the high speed impact of the plates. Deformation during the collision is limited to a very narrow thickness close to the surface (Fig. 10). Thereby, the hardness value decreases as the distance from the interface increases [42]. Also, at higher values of explosive ratio, higher levels of plastic deformation and thus higher hardness values are achieved [43].

Microhardness profiles after rolling process of specimens with R=1.6 are presented in Fig. 11(b). During rolling, the plastic deformation results in a hardness increase compared to the hardness of the as-welded plate. By increasing the thickness reduction, more obvious increase in hardness values can be seen because of the higher strain and excessive work hardening. However, the increase is more profound for copper layer due to its lower stacking fault energy (~ 250 and 90 mj/m^2 for Al and Cu, respectively) [44]. On the other hand, a higher relative hardness increase occurs in the middle of the plates compared to the interfacial areas, especially for copper. This is probably owing to the lower degree of plastic deformation in the middle of plates during welding which allows higher hardening

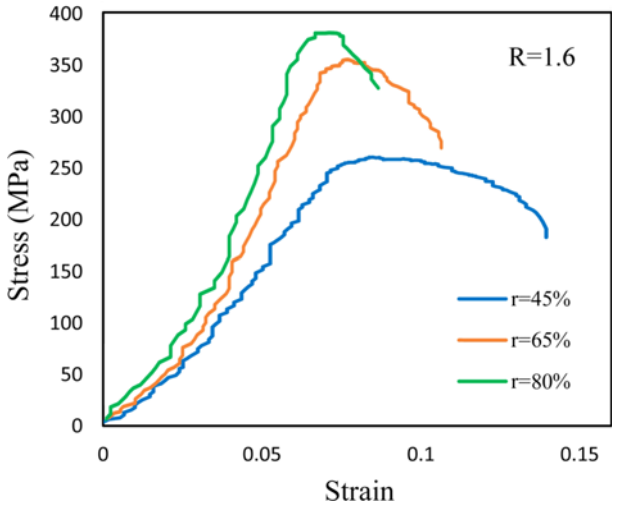

Fig. 12. True stress-strain curves for Al-Cu-Al laminated plates after explosive welding and subsequent rolling process.

in these areas by cold rolling. Therefore, a more uniform hardness variation is obtained after rolling process.

3.3. Tensile tests

Engineering stress-strain curves of specimens after rolling at different thickness reductions are plotted in Fig. 12. According to this figure, considerable increase in yield and tensile strength is reached by increasing the thickness reduction. However, elongation of the welded plate is reduced. It has been reported that strength variation in laminated composites is controlled by two main strengthening mechanisms; strain/work hardening by dislocations entanglement and grain boundary strengthening or grain refinement based on Hall-Petch relation [44]. In explosive welding process which includes high pressure impact, increased strength might originate from severe grain refinement near the interface (Fig. 10(a) and (b)). During subsequent rolling process, work hardening is the dominant strengthening mechanism. Elongated structure observed in Fig. 10(c) for rolled specimens are a good evidence for significant work hardening. Previous results have shown that during rolling process, grain refinement has a less contribution in the increase of tensile strength compared to work hardening mechanism

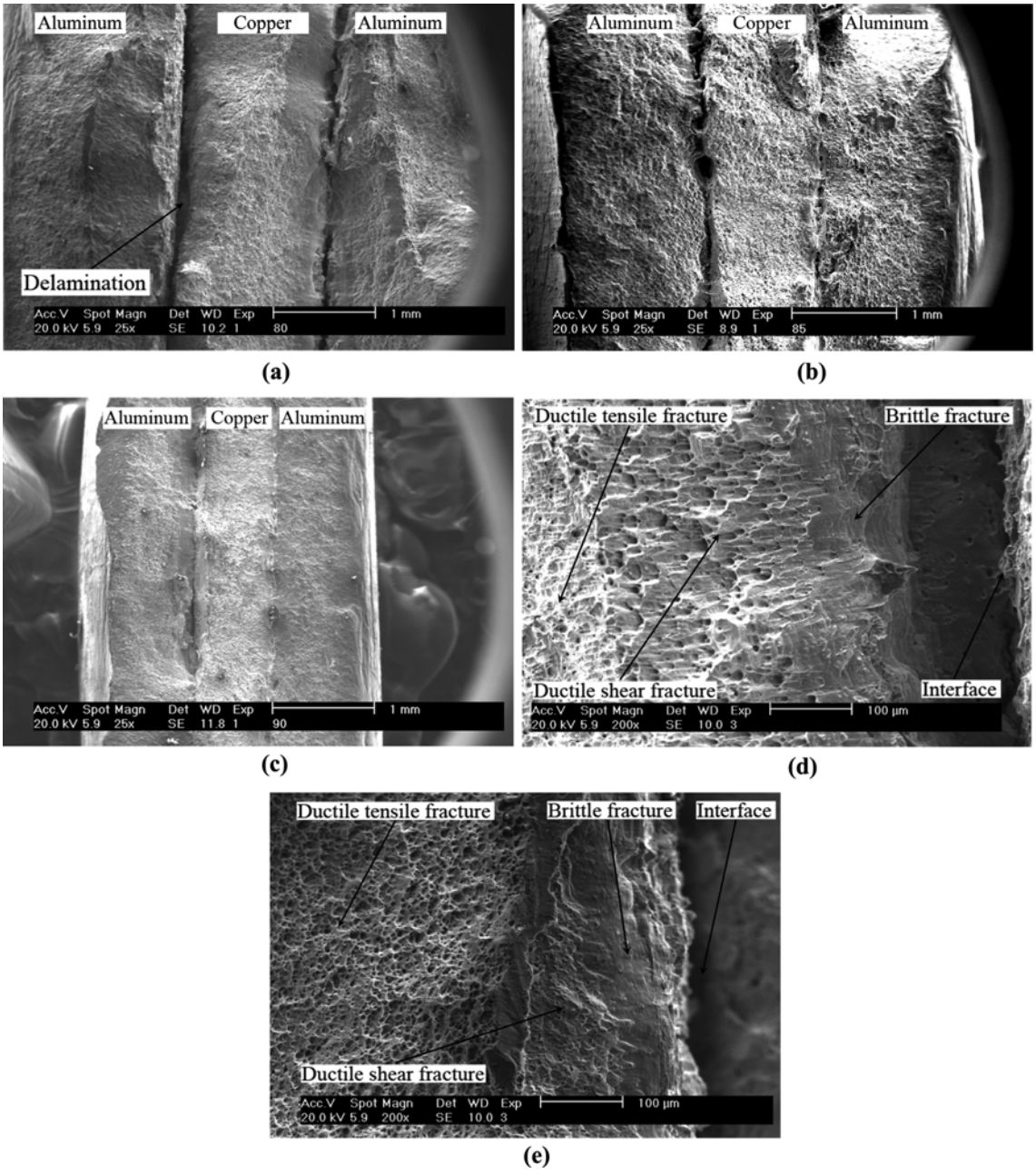

Fig. 13. Secondary electron images of fracture surface of tensile specimens after explosive welding with R=1.6 and rolling at thickness reductions of (a) 45%, (b) 55%, (c) 80%, (d) and (e) higher magnification of a and c, respectively.

[44,45]. Furthermore, elongation decreases intensively because of the reduction of dislocations mobility or lower rate of hardening [46].

To investigate the fracture mechanism, SEM macro and micro images in secondary electron (SE) mode were taken from the fracture surface of the tensile test specimens. Fig. 13(a) indicates significant partial delamination at the interface of specimen rolled under lower thickness reduction [44]. However, less bond breakage is observed for specimens rolled at higher reductions (Figs. 13(b) and (c)). This implies that rolling process can be effectively used to improve bonding strength of explosively welded materials. Better bonding properties at high rolling reductions might be related to the improved mechanical locking and also higher L_{eff} value arising from the IMC fragmentation and formation of secondary bonds [47].

According to Fig. 13(d), three different regions can be discerned on the fracture surface of specimen rolled with r=45% presenting both ductile dimples and quasi cleavage features. The shape of dimples as the typical fracture morphology of ductile materials changes with the stress condition. Deep equiaxed dimples are formed under normal stress; whereas, elongated shallow dimples are an indication of shear stress [48]. In tensile test, the uniform deformation of laminated composite with good bonding is preserved by the interfacial region between individual layers. However, owing to the low ductility of this region containing some brittle intermetallic phases and severely deformed grains, cleavage fracture occurs without any dimples. In this situation, some cracks are initiated at the interface and propagate along the tensile direction. Earlier studies have also reported that rupture of explosively welded samples are accelerated by the presence of IMCs [29]. After partial bond separation, elongation under uniaxial load continues and equiaxed dimples are created away from the interface by micro void coalescence. Between the ductile and brittle fracture regions, there is a narrow transitional band including shallow elongated dimples suggesting that they are formed by shear rupture mechanism. The final fracture takes place by shearing of the inter-void ligaments in this region [44,49]. In addition, comparing Figs. 13(d) and (e) reveals that the shear fracture is diminished by increasing the rolling thickness reduction. This might be due to the more uniformity in mechanical properties obtained by rolling at high thickness reductions as it was previously observed for microhardness measurements (Fig. 11).

3.4. Tensile-shear tests

Tensile-shear tests were performed to investigate the effect of rolling on the bonding strength of explosively welded plates. The results of the tests are summarized in Fig. 14. The bonding strength of as-welded specimens are 85, 107 and 64 MPa under explosive ratios of R=1, R=1.6 and R=2.2, respectively. For R=1.6, a lower L_{eff} is achieved compared to R=1 (Fig. 9(b)), but higher wavy interface and better

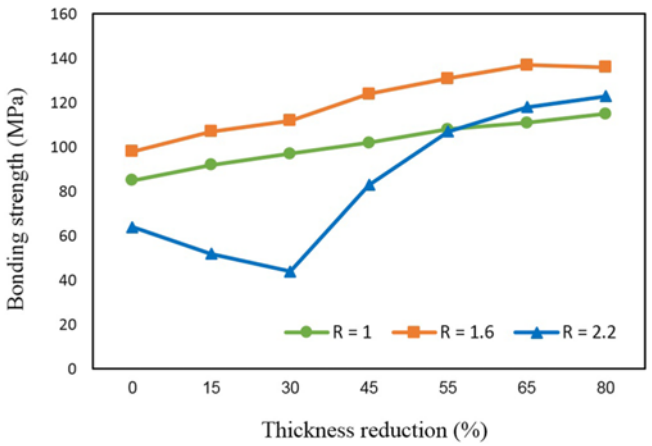

Fig. 14. Bonding strength of explosively welded and cold rolled joints measured by the tensile-shear test.

mechanical locking improves the bonding strength [22,50]. Accordingly, it seems that a compromise between L_t and L_{eff} must be reached to obtain the best bonding properties. On the other hand, the results for R=2.2 contradicts with the earlier belief that bonding strength always increases by increasing the explosive ratio [51]. The reason of this observation includes intermetallic formation and associated defects such as cooling cavities (Fig. 5) as well as lower L_{eff} values. Therefore, it is rational that by increasing the explosive ratio to R=2.2, hence acquiring higher fraction of weak and brittle Al/Cu-IMC interface, the overall bonding strength is reduced.

For specimens welded using explosive ratios of R=1 and R=1.6, shear strength enhances by increasing the thickness reduction. This might be due to the flattening of vortices and entrapment of metals which provide a better mechanical interlocking. Also, higher tensile strength (Fig. 12) for rolled specimens can be held responsible for improvement in bonding strength [52,53].

A different behavior is detected for specimen welded with R=2.2. Under this condition, increasing the rolling thickness reduction up to r=30% leads to considerable decrease in bonding strength. However, when thickness reduction exceeds this value, bonding strength is intensified. This behavior can be explained by comparing Figs. 9(b) and 14. For R=2.2, the effects of rolling on bonding strength and L_{eff} are almost similar. Beyond 30% reduction, fragmentation of IMCs along with getting further away cause an increase in unbonded areas at the interface and consequently lowers the L_{eff}. Indeed, intermetallic cracking and void creation at the interface reduce the bonding strength. However, extrusion of metals results in the formation of new Al-Cu interface and therefore enlarges the L_{eff}. Higher length of this interface can increase the bonding strength and it seems that L_{eff} can be used to predict the bonding strength variations.

Figure 15 illustrates the SEM-backscattered electron images of the fracture surface on the copper side of tensile-shear

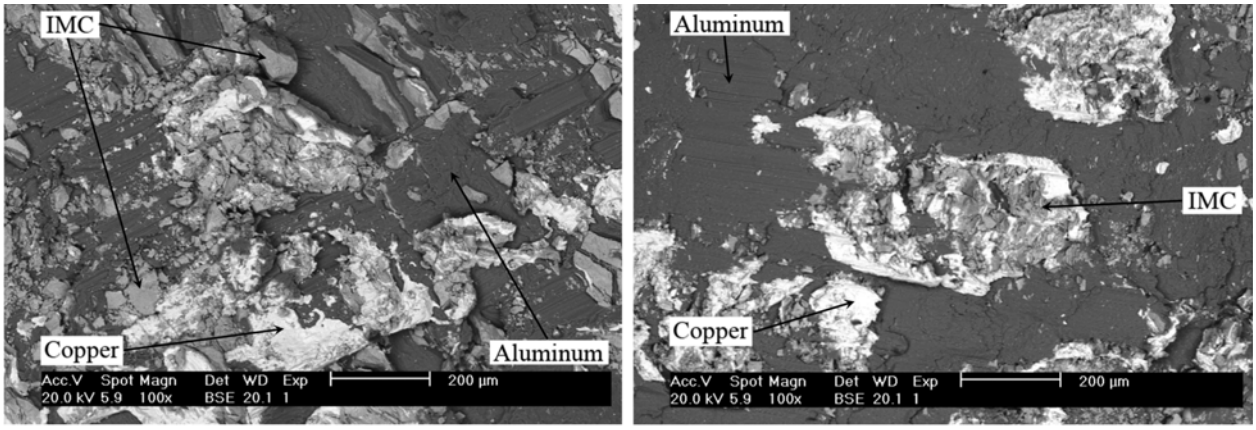

Fig. 15. SEM-backscattered electron images of tensile-shear test specimens with R=2.2 explosive ratio and thickness reduction of (a) r=45% and (b) r=65%.

test specimen for R=2.2 explosive ratio. Regarding this figure, aluminum is the major part on the surface of the copper layer. This reveals that fracture takes place mostly in aluminum rather than exactly at the interface. Thereby, it can be stated that the interface is stronger than aluminum [26]. Because of higher strength of aluminum at higher thickness reductions, obtaining better bonding strength might be expected.

In addition to aluminum (dark color) and traces of copper (bright color), regions with light grey color are observed which were characterized as intermetallic compounds. Existence of IMCs at the interface accelerate the nucleation and propagation of micro-cracks, and accordingly leads to the reduction of bonding strength [29]. Comparing Figs. 15(a) and (b) indicates that the amount and size of IMCs decrease with increasing the thickness reduction. This confirms the higher fraction of Al-Cu interface and is in agreement with the value of effective bond length. Lower fraction of IMCs at the interface can increase the bonding strength.

4. CONCLUSIONS

In this study, the effect of cold rolling process on different interface morphologies of explosively welded Al-Cu-Al laminated composite was investigated. Based on the obtained results, the main conclusions can be summarized as follows:

(1) A smooth interface is observed at lower explosive ratio (R=1), however the interface transforms to a wavy state at higher explosive ratio (R=1.6) due to the higher collision pressure. At the highest explosive ratio (R=2.2), local melting and formation of intermetallic compounds (IMCs) with cracking and cooling cavities occur.

(2) For wavy interface, subsequent rolling process results in flattening and joining of adjacent vortices as well as formation of IMC islands. For interface with melted layer, increasing the thickness reduction up to 30% leads to fragmentations of IMCs. After that, extrusion of virgin metals between IMCs takes place accompanied by formation of secondary bonds.

(3) The measured hardness values of the welded specimens are higher than those of the original materials. The maximum hardness value is recorded near the interface of the copper and aluminum layers. Also after rolling, higher hardness values are reached. The relative hardness increase near the interface is lower because of the severe hardening during explosive welding.

(4) Tensile tests reveal considerable increase in yield and ultimate strength along with reduction in elongation by increasing the rolling thickness reduction. Furthermore, less significant bond separation of specimens rolled under high thickness reduction indicates partial improvement in the bonding strength.

(5) The highest bonding strength is achieved for wavy interface (R=1.6). This is due to the higher bonding area and low amounts of IMCs. For this situation, the best compromise between total and effective bond length is obtained.

(6) For specimens welded using explosive ratios of R=1 and R=1.6, the bonding strength increases with increasing the rolling thickness reduction. Whilst, for R=2.2, bonding strength decreases up to a threshold thickness reduction and then increases owing to the formation of secondary bonds.

ACKNOWLEDGEMENTS

The authors would like to express their appreciation to the personnel of metal forming laboratory of Sharif University of Technology and also metallography laboratory of Iran University of Science and Technology for their cooperation throughout this research.

REFERENCES

1. X. K. Peng, R. Wuhrer, G. Heness, and W. Y. Yeung, *J. Mater. Sci.* **34**, 2029 (1999).

2. D. Manesh and K. Taheri, *Mech. Mater.* **37**, 531 (2005).
3. R. Uscinowicz, *Compos. Part B* **44**, 344 (2013).
4. T. Mai and A. Spowage, *Mater. Sci. Eng. A* **374**, 224 (2004).
5. H. D. Manesh and A. K. Taheri, *J. Alloy. Compd.* **361**, 138 (2003).
6. L. Y. Sheng, F. Yang, T. F. Xi, C. Lai, and H. Q. Ye, *Compos. Part B* **42**, 1468 (2011).
7. G. P. Chaudhari and V. Acoff, *Compos. Sci. Technol.* **69**, 1667 (2009).
8. C. Xia, Y. Li, U. Puchkov, S. Gerasimov, and J. Wang, *Vacuum* **82**, 799 (2008).
9. W. B. Lee, K. S. Bang, and S. B. Jung, *J. Alloy. Compd*. **390**, 212 (2005).
10. F. Findik, *Mater. Des*. **32**, 1081 (2011).
11. A. Loureiro, R. Mendes, J. B. Ribeiro, R. M. Leal, and I. Galvão, *Mater. Des.* **95**, 256 (2016).
12. A. A. Akbari Mousavi and S. T. S. Al-Hassani, *J. Mech. Phys. Solids* **53**, 2501 (2005).
13. A. Bahrani, T. Black, and B. Crossland, *Proc. Roy. Soc. A. Math. Phy. Sci.* **296**, 123 (1967).
14. A. Ben-Artzy, A. Stern, N. Frage, V. Shribman, and O. Sadot, *Int. J. Impact Eng.* **37**, 397 (2010).
15. G. R. Cowan, O. R. Bergmann, and A. H. Holtzman, *Metall. Mater. Trans B* **2**, 3145 (1971).
16. H. El-Sobky and T. Blazynski, *Proc. 5th International Conference on High Energy Rate Fabrication*, pp. 1-21, Denver, Colorado.
17. M. M. H. Athar and B. Tolaminejad, *Mater. Des.* **86**, 516 (2015).
18. S. A. A. A. Mousavi and P. Farhadi Sartangi, *Mater. Des*. **30**, 459 (2009).
19. M. Acarer, B. Gülenç, and F. Findik, *Mater. Des.* **24**, 659 (2003).
20. A. Durgutlu, H. Okuyucu, and B. Gulenc, *Mater. Des.* **29**, 1480 (2008).
21. B. Wronka, *J. Mater. Sci.* **45**, 3465 (2010).
22. S. A. A. A. Mousavi, S. T. S. Al-Hassani, and A. G. Atkins, *Mater. Des.* **29**, 1334 (2008).
23. H. R. Z. Rajani and S. A. A. A. Mousavi, *Mater. Sci. Eng. A* **556**, 454 (2012).
24. K. Hokamoto, T. Izuma, and M. Fujita, *Metall. Trans. A* **24**, 2289 (1993).
25. T. Inal and C. Zimmerly, *9th International Metallurgy and Materials Congress*, pp.751-764, Istanbul Turkey.
26. R. Kacar and M. Acarer, *J. Mater. Proc. Technol.* **152**, 91 (2004).
27. A. G. Mamalis, N. M. Vaxevanidis, A. Szalay, and J. Prohaszka, *J. Mater. Proc. Technol.* **44**, 99 (1994).
28. A. G. Mamalis, N. M. Vaxevanidis, and A. Szalay, *Int. J. Mach. Tool. Manu*. **36**, 1033 (1996).
29. M. Asemabadi, M. Sedighi, and M. Honarpisheh, *Mater. Sci. Eng. A* **558**, 144 (2012).
30. A. G. Mamalis, A. Szalay, N. M. Vaxevanidis, and D. E. Manolakos, *J. Mater. Proc. Technol.* **83**, 48 (1998).
31. F. Grignon, D. Benson, K. S. Vecchio, and M. A. Meyers, *Int. J. Impact Eng.* **30**, 1333 (2004).
32. Y. Kaya and N. Kahraman, *Mater. Des.* **52**, 367 (2013).
33. M. Hammerschmidt and H. Kreye, *J. Metals* **37**, pp. 12-21 (1984).
34. H. Xu, C. Liu, V. V. Silberschmidt, S. S. Pramana, T. J. White, Z. Chen, and V. L. Acoff, Acta Mater. **59**, 5661 (2011).
35. A. G. Mamalis, N. M. Vaxevanidis, and A. Szalay, *J. Mater. Proc. Technol*. **45**, 407 (1994).
36. L. Vaidyanath, M. Nicholas, and D. Milner, *Brit. Weld. J.* **6**, 13 (1959).
37. R. Jamaati and M. R. Toroghinejad, *Mater. Sci. Eng. A* **527**, 2320 (2010).
38. N. Bay, *J. Manuf. Sci. Eng.* **101**, 121 (1979).
39. J. Yong, P. Dashu, L. Dong, and L. Luoxing, *J. Mater. Proc. Technol.* **105**, 32 (2000).
40. G. Y. Tzou and M. N. Huang, *J. Mater. Proc. Technol.* **140**, 622 (2003).
41. M. Movahedi, H. R. Madaah-Hosseini, and A. H. Kokabi, *Mater. Sci. Eng. A* **487**, 417 (2008).
42. B. Gulenc, *Mater. Des.* **29**, 275 (2008).
43. A. Durgutlu, B. Gülenç, and F. Findik, *Mater. Des.* **26**, 497 (2005).
44. M. Eizadjou, A. Kazemi Talachi, H. Danesh Manesh, H. Shakur Shahabi, and K. Janghorban, *Compos. Sci. Technol*. **68**, 2003 (2008).
45. K. T. Park, H. J. Kwon, W. J. Kim, and Y. S. Kim, *Mater. Sci. Eng. A* **316**, 145 (2001).
46. D. Terada, S. Inoue, and N. Tsuji, *J. Mater. Sci.* **42**, 1673 (2007).
47. S. Nambu, M. Michiuchi, J. Inoue, and T. Koseki, *Compos. Sci. Technol.* **69**, 1936 (2009).
48. J. Wang, P. Zhang, Q. Duan, G. Yang, S. Wu, and Z. Zhang, *Adv. Eng. Mater.* **12**, 304 (2010).
49. X. Li, G. Zu and P. Wang, *Mater. Sci. Eng. A* **575**, 61 (2013).
50. N. Kahraman, B. Gülenç, and F. Findik, *J. Mater. Proc. Technol.* **169**, 127 (2005).
51. B. Crossland and J. Williams, *Metall. Rev.* **15**, 79 (1970).
52. X. Li, G. Zu and P. Wang, *Mater. Sci. Eng. A* **562**, 96 (2013).
53. H. R. Akramifard, H. Mirzadeh, and M. H. Parsa, *Mater. Sci. Eng. A* **613**, 232 (2014).